Laser Chem. 1988, Vol. 9, pp. 47–62

A Test for Bottlenecks in the Vibrational Relaxation of CH_3Cl and CH_3Br by Ar

KENNETH M. BECK and ROBERT J. GORDON

Department of Chemistry, University of Illinois at Chicago, Chicago, Illinois 60680

(Received January 5, 1988; in final form March 31, 1988)

The method of time-resolved optoacoustics was used to measure the rate of vibrational relaxation of $CH_3Cl(v_6)$ and $CH_3Br(v_6)$ by Ar. The pressure pulses generated by the relaxing gas revealed that the rate of production of translational energy from $v_6 = 1$ is approximately twice the decay rate of IR fluorescence from $v_3 = 1$. No evidence was found for a previously proposed bottleneck in rotational relaxation, which would have resulted in an acoustic relaxation rate slower than the fluorescence decay. The faster rates observed here can be explained qualitatively by a rapid energy release from energy levels above v_3 which precedes the IR fluorescence. A simple three-level model, however, is unable to explain our observations quantitatively.

KEY WORDS: Energy transfer, vibrational relaxation, VT transfer, hydrogen halides.

I. INTRODUCTION

Vibrational relaxation of polyatomic molecules diluted in a bath gas is a complicated process involving many elementary steps, including intermode coupling (IC) of different normal modes, vibration-to-rotation (VR) energy transfer connecting specific vibrational and rotational eigenstates, rotation-to-translation energy transfer (RT), and vibration-to-translation (VT) energy transfer. These steps are shown schematically in the following diagram:

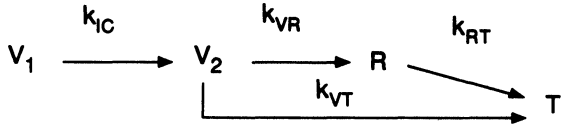

In this very simplified picture V_1 represents the vibrational state(s) initially prepared by some physical or chemical process (e.g. absorption of a photon, chemical reaction, or inelastic collision with an energetic particle), V_2 is a set of "doorway" vibrational states, R denotes the rotational degrees of freedom of the excited molecule, and T denotes the translational modes of the bath.

The net result of this mechanism is conversion of vibrational energy into heat. If any of the steps is substantially slower than the others it may act as a bottleneck in the relaxation process. For example, if $k_{RT} \gg k_{VT}$ and $k_{RT} \ll k_{VR}$, a rotational bottleneck will result. This could occur for molecules with small moments of inertia or with large rotational quantum numbers, such that the energy spacing of adjacent levels is large compared with kT. An example of a rotational bottleneck is the relaxation of CN($X, v = 0$) by Ar and Kr.[1] Alternatively, a vibrational bottleneck can occur if $k_{VT}, k_{VR} \ll k_{IC}$, with the vibrational relaxation of the lowest excited vibrational level being the rate-limiting step.

In order to identify the existence of such bottlenecks it is necessary to measure the rate constants for each elementary step. To construct a complete "energy map" a variety of different experimental measurements is required. Much of what is known about the relaxation of small polyatomic molecules has been learned from infrared fluorescence experiments. By measuring the emission from different vibrational modes and performing eigenvalue analyses of the rise and decay rates of the emission, it has been possible to construct detailed maps of the flow of energy in a variety of three, four, and five atom molecules. These studies, while very informative, are necessarily incomplete since they do not distinguish between competing radiationless transitions.

The limitations of IR fluorescence measurements are illustrated by the relaxation of CH_3Cl_6 and CH_3Br_6 by Ar. In these experiments the ν_6 mode was excited with a CO_2 laser and emission was observed from ν_3 and various overtone and combination bands. (See Figure 1 for abbreviated energy level diagrams.) The observation of a common decay rate for all the emitting levels for a given collision pair suggests a

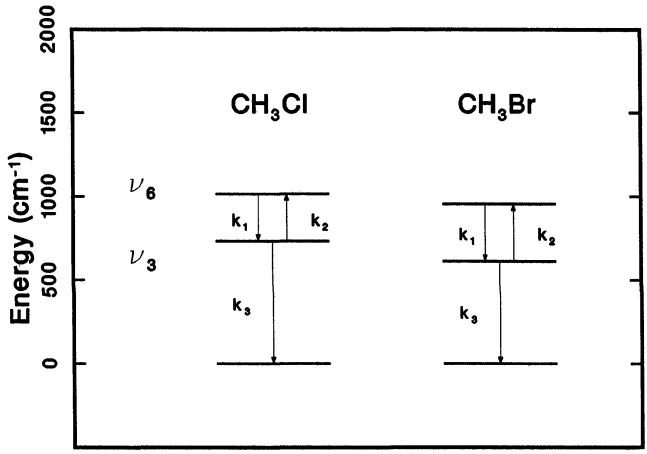

Figure 1 Abbreviated energy level diagrams for CH_3Cl and CH_3Br. In both cases the v_6 mode is excited by the laser. The arrows depict the rate constants used in the three-level kinetic model.

single rate-limiting step. This step is presumed to be a combination of VT and VR relaxation of v_3, although some direct relaxation of v_6 may also contribute. While the fluorescence experiment cannot distinguish between VR and VT relaxation, the insensitivity of the rate constant to reduced mass suggests a predominance of the VR process.[2] This interpretation is bolstered by the fact that the rotational velocity about the principal axis is much larger than the relative collision velocity for the heavier partners including Ar. If indeed $k_{VR} \gg k_{VT}$ then the possibility of a rotational bottleneck must be considered.

Another potential bottleneck exists in the vibrational relaxation of v_3. Although fluorescence from v_6 was not observed, k_{IC} can be determined from the rise rate of the v_3 emission. While this rate constant was determined for neat CH_3Cl and CH_3Br, it could not be extracted from Stern-Volmer plots for binary gas mixtures. Nevertheless, it is very likely that k_{VT}, $k_{VR} \ll k_{IC}$, raising the possibility of a vibrational bottleneck in v_3.

One way to verify the existence of such bottlenecks is to measure directly the rate at which energy is deposited into translational degrees of freedom. In general, one would expect this rate to differ from the v_3 decay rate. If an RT bottleneck exists the translational heating rate would be slower than the fluorescence decay rate (i.e. energy leaving

ν_3 is "trapped" in a dark state), whereas for a VT/VR bottleneck it should be faster than the fluorescence rate. Such an experiment was in fact performed by Schuurman and Wegdam,[4] who used both a spectrophone and a technique which we call resonant optoacoustics (ROA). In the latter method the gas sample is irradiated with a pulsed laser in a small cylindrical cell. The acoustic signal is detected with a microphone mounted flush with the curved wall. This signal consists of a sequence of oscillations produced by the radial and longitudinal resonances of the cell. The envelope of these oscillations has a rise time corresponding to the time constant for energy transfer from the excited molecules to the bath gas.

Schuurman and Wegdam applied these methods to the relaxation of CH_3I, CH_3Br, CH_3Cl and CH_3F by Xe,[4b] Kr, Ar, Ne and He — a total of 20 binary mixtures. Their results were most unusual. They reported energy decay rates which differed strongly from the IR fluorescence results, being in some cases as much as 9 times slower (CH_3I + He) and in others as much as 11 times faster (CH_3F + Kr). The rate constants measured acoustically varied by a factor of only 3.3 in going from the slowest to the fastest system, whereas the fluorescence decay rates varied by a factor of 255.

Because of the surprising nature of these results we decided to re-examine two of the systems using the method of time-resolved optoacoustics (TROA). In this technique a large acoustic chamber is used and a fast piezoelectric transducer is placed normal to the laser beam far from the chamber walls. With this geometry a single acoustic wave is intercepted long before a standing wave pattern is formed. The characteristic shape of such a wave is a positive-going condensation pulse with amplitude I_+ followed by a negative-going rarefaction pulse of amplitude I_-. The quantity I_-/I_+ is a direct measure of the vibrational relaxation rate. This ratio is approximately unity when the relaxation time constant τ is much smaller than τ_{sonic}, the time required for the acoustic wave to traverse the radius of the laser beam, while in the limit of very slow relaxation I_-/I_+ approaches zero.

The TROA method has been tested extensively by measuring the relaxation rates for a number of systems (OCS + Ar,[5] OCS + He,[5] SF_6 + Ar,[6,7] and C_6F_5H + Ar[6]) for which the rate constants vary by a factor of 100. The results for a variety of experimental methods (TROA, ROA, IR fluorescence, and Hg tracer absorption) were compared and were all found to agree within experimental error. The TROA tech-

nique should therefore provide an independent test for possible bottlenecks in the relaxation of methyl halides by rare gases.

II. KINETIC MODEL

The relation between the acoustic amplitude ratio I_-/I_+ and the relaxation time τ depends critically on the mathematical form of the source function, which describes the rate at which energy is deposited into the bath gas. Since determination of this function requires a model of the relaxation mechanism, we will first discuss the anticipated behavior of CH_3Cl and CH_3Br before presenting the experimental results.

The simplest model of CH_3Cl and CH_3Br relaxation involves the three lowest vibrational levels shown in Figure 1. The relaxation mechanism consists of the following steps:

$$CH_3X(v_6) + Ar \underset{k_2^{XA}}{\overset{k_1^{XA}}{\rightleftharpoons}} CH_3X(v_3) + Ar$$

$$CH_3X(v_3) + Ar \underset{k_4^{XA}}{\overset{k_3^{XA}}{\rightleftharpoons}} CH_3X(0) + Ar$$

and analogous steps for self-relaxation with rate constants k_i^{XX}, where X = Cl or Br. Since $k_4^{XA}/k_3^{XA} = 0.030$ for CH_3Cl and 0.053 for CH_3Br, we chose to ignore the last step. A further approximation in our model is to ignore the small temperature rise of the bath gas resulting from V → R/T energy transfer. The maximum that this could be is 2.0 to 4.8 K for CH_3Cl and 3.9 to 6.8 K for CH_3Br, assuming that all the released energy remains within the laser beam.

With these approximations, the varying concentrations of $CH_3X(v_6)$ and $CH_3X(v_3)$ may be determined analytically. Denoting these concentrations as $X(t)$ and $Y(t)$, and assuming $Y(t=0) = 0$, we obtain the well-known result[2]

$$X(t) = Ae^{-\lambda_1 t} + Be^{-\lambda_2 t} \tag{1}$$

$$Y(t) = e^{-\lambda_2 t} - e^{-\lambda_1 t} \tag{2}$$

The eigenvalues λ_1 and λ_2 and the amplitudes A and B can be expressed in terms of the rates R_1, R_2, and R_3, where

$$R_i = k_i^{XA}\,[\mathrm{Ar}] + k_i^{XX}\,(\mathrm{CH_3X}] \tag{3}$$

From detailed-balancing, $R_2/R_1 = 0.51$ for CH_3Cl and 0.38 for CH_3Br at 300 K. The amplitudes are given by the relations

$$A = R_2/(\lambda_1 - R_1) \tag{4}$$

and

$$B = R_2/(R_1 - \lambda_2) \tag{5}$$

while the eigenvalues are

$$\lambda_{1,2} = \tfrac{1}{2}(R_1 + R_2 + R_3)\{1 - [1 - 4R_1R_2/(R_1 + R_2 + R_3)^2]^{1/2}\} \tag{6}$$

The plus sign in Eq. (6) corresponds to the fast rate λ_1, and the minus sign to the slow rate λ_2.

An important physical property of the eigenvalues is that they have a nearly linear dependence on buffer gas pressure P_A for small mole fractions of CH_3X. This can be seen by expanding the eigenvalues in Taylor series. To an excellent approximation

$$\lambda_1 = (R_1 + R_2 + R_3) - R_1R_3/(R_1 + R_2 + R_3) \tag{7}$$

and

$$\lambda_2 = R_1R_3/(R_1 + R_2 + R_3) \tag{8}$$

We can further rearrange Eq. (8) to the form

$$\lambda_2 = R_3\left(\frac{R_1}{R_1 + R_2}\right)\left(\frac{R_1 + R_2}{R_1 + R_2 + R_3}\right)$$

where the only non-linearity in P_A arises from the last factor. The exact derivative $d\lambda_2/dP_A$ varies by ~1% between 30 and 100 Torr. Another important property of the analytic solution is the limiting behavior for $R_2 \gg R_3$. In this limit $A \to 1$ and $B \to R_2/R_1$.

The total vibrational energy of the relaxing molecules is given by

$$E(t) = E_6X(t) + E_3Y(t) \tag{10}$$

where $E_i = h\nu_i$. Substituting Eqs. (1) and (2) into Eq. (10) we obtain

$$E(t) = (AE_6 - E_3)e^{-\lambda_1 t} + (BE_6 + E_3)e^{-\lambda_2 t} \tag{11}$$

It is convenient to renormalize the energy function as

$$E(t) = f_1 e^{-\lambda_1 t} + f_2 e^{-\lambda_2 t} \tag{12}$$

where $f_2 + f_2 = 1$.

III. ANALYSIS OF THE OPTOACOUSTIC SIGNAL

The quantity $E(t)$ is the temporal part of the source function which generates the optoacoustic signal, $I(t)$. The acoustic waveform can be obtained by solving the linearized wave equation, using either a Fourier expansion[8,9] or a Green's function analysis.[9] The latter is especially convenient to implement for a tophat laser pulse. In these calculations it is useful to define the reduced time, $s = t/\tau_{\text{sonic}}$, where in the present experiments $\tau_{\text{sonic}} = 16.9$ μs. Defining $\varepsilon_i = \lambda_i \tau_{\text{sonic}}$, we obtain

$$E(s) = f_1 e^{-\varepsilon_1 s} + f_2 e^{-\varepsilon_2 s} \tag{13}$$

It is then straightforward to show that

$$I(s) = (f_1\varepsilon_1 + f_2\varepsilon_2)G(s,r) - \int_0^s (f_1\varepsilon_1^2 e^{-\varepsilon_1 s'} + f_2\varepsilon_2^2 e^{-\varepsilon_2 s'}(G(s-s',r)ds' \tag{14}$$

where $G(s,r)$ is the Green's function for a cylindrical tophat.[5]

A model calculation of the TROA signal is shown in Figure 2. In this calculation fixed values of $\varepsilon_1 = 10$ and $\varepsilon_2 = 1$ where chosen, while f_1 was allowed to vary from 0 to 1. This figure illustrates how $I(s)$ varies continuously between the two single-exponential limits. Also illustrated is an interesting induction effect at low values of f_1. The calculated waveforms show that as f_1 increases from zero the condensation and rarefaction peaks both become steeper. However, the amplitude ratio does not begin to grow until f_1 exceeds a value of ~0.2, and only for $f_1 > 0.3$ is there a substantial increase in I_-/I_+. This is shown more clearly in Figure 3 where I_-/I_+ is plotted as a function of f_1. A consequence of this effect is that if the pre-exponential factor of the fast component is less than 40% of that of the slow component, then the amplitude ratio of the TROA signal will lock onto the value for the larger of the two time constants. While in principle the presence of the faster component can still be detected from the shape of the rarefaction wave, this may be difficult because of ringing in the detector which follows the negative pulse.

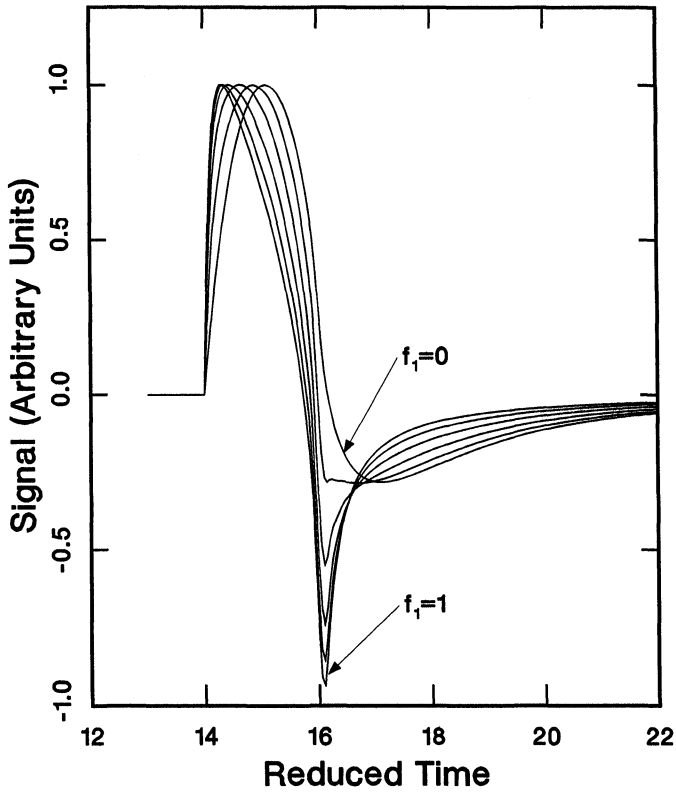

Figure 2 Calculated optoacoustic signal for a tophat geometry and a double exponential temporal function. The fast component has a reduced decay rate of $\varepsilon_1 = 10$ and a pre-exponential factor f_1, while the slow component has a decay rate of $\varepsilon_2 = 1$ and a pre-exponential factor of $1-f_1$. The slow decay rate corresponds to 2.1 Torr of CH_3Cl and 80.3 Torr of Ar.

The qualitative behavior of the TROA signal for CH_3Cl and CH_3Br can be readily calculated. From Eqs. (4–10) we find that the maximum value that f_1 can achieve in the limit of very rapid ν_6–ν_3 coupling is given by

$$f_{max} = (1 + K)^{-1}(1 - E_3/E_6) \tag{15}$$

where detailed balancing gives

$$K = R_2/R_1 = 2 \exp\{-(E_6-E_3)/kT\} \tag{16}$$

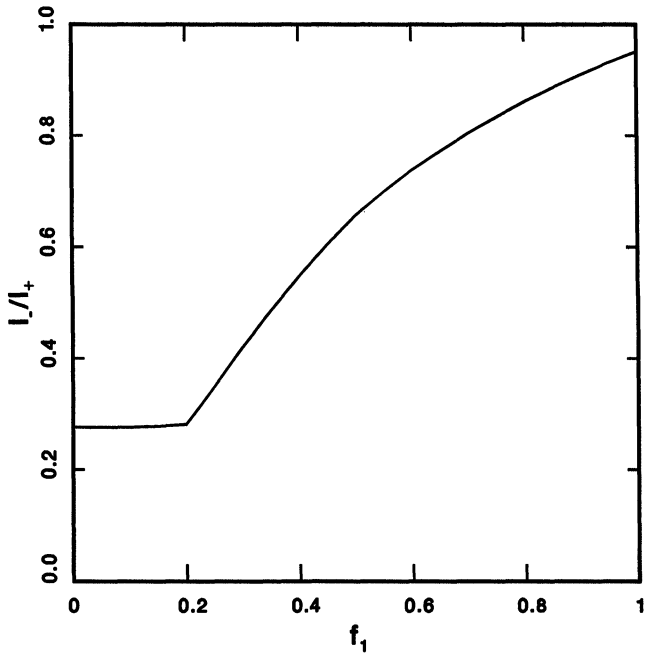

Figure 3 Predicted optoacoustic amplitude ratio for the biexponential source function used in Figure 2.

For CH_3Cl and CH_3Br we obtain $f_1 < 0.18$ and 0.26, respectively. We conclude that a plot of I_-/I_+ vs. ε for a single exponential decay is appropriate for analyzing the relaxation of these molecules, provided that the three-level model is correct. Moreover, the eigenvalues obtained from TROA for the decay of $E(t)$ and from IR fluorescence for decay of the v_3 population should be identical.

IV. EXPERIMENTAL METHODS

The TROA technique has been described in earlier papers,[7,8] and a detailed discussion will be published in a separate report.[5] As before, the acoustic chamber was a stainless steel cylinder (31 cm i.d., 30 cm long) fitted with KCl windows on each face. The chamber was irradiated with a CO_2 TEA laser tuned to the P(26) line of the 10.6 μm

band (1041 cm^{-1}) for CH_3Cl and the R(14) line of the 10.6 μm band (972 cm^{-1}) for CH_3Br. The laser had a "tophat" pulse shape with a radius of 0.54 cm. The temporal width of the laser pulse was 150 ns FWHM with a tail 0.5 μs long containing ~15% of the energy. The laser fluence was attenuated with CaF_2 flats and was 85 mJ/cm^2 in the CH_3Cl runs and 138 mJ/cm^2 for CH_3Br. The average number of photons absorbed per molecule was 0.10 for CH_3Cl and 0.12 for CH_3Br. In trial experiments with CH_3Cl + Ar we found that I_-/I_+ was independent of laser intensity for fluences between 21 and 220 mJ/cm^2.

The TROA signal was detected with a PZT piezoelectric crystal (International Transducer PK-14) having a 1.2 MHz response at 3db attenuation. The transducer was mounted normal to the laser beam, between 6.3 and 8.7 cm from the cell axis. The signal was amplified by a factor of 10^3 to 5×10^3 with a DC coupled amplifier (1 MHz at 3db), digitized with a transient recorder (100 MHz, 80 ns gate), and averaged for 10^3 shots on a microcomputer.

The speed of sound, which is needed to calculate τ_{sonic}, was determined by measuring the arrival time of the acoustic pulse (i.e. from the leading edge of the condensation wave), and also from the width of the condensation wave at its base. Both values were in close agreement with the known speed of sound of Ar.

The experiments were performed with constant partial pressures of the methyl halides (2.11 Torr of CH_3Cl and 2.96 Torr of CH_3Br), while the Ar pressure was varied. The gases were thoroughly mixed in advance in a pyrex bulb. CH_3Cl (Matheson, 99.5%) and CH_3Br (Matheson, 99.5%) were purified by several cycles of vacuum distillation, with only the middle fractions retained. Argon (Matheson, 99.999%) was used without further purification. The acoustic chamber was filled statically with the gas mixture just prior to each run, using a capacitance manometer to measure the pressure.

V. RESULTS

A typical TROA waveform is shown in Figure 4, which illustrates the condensation and rarefaction amplitudes I_- and I_+. The measured amplitude ratios for CH_3Cl + Ar and CH_3Br + Ar are plotted in Figure 5 as functions of Ar partial pressure. As explained in Sections II and III, for a three-level model the pressure dependence of I_-/I_+ is the

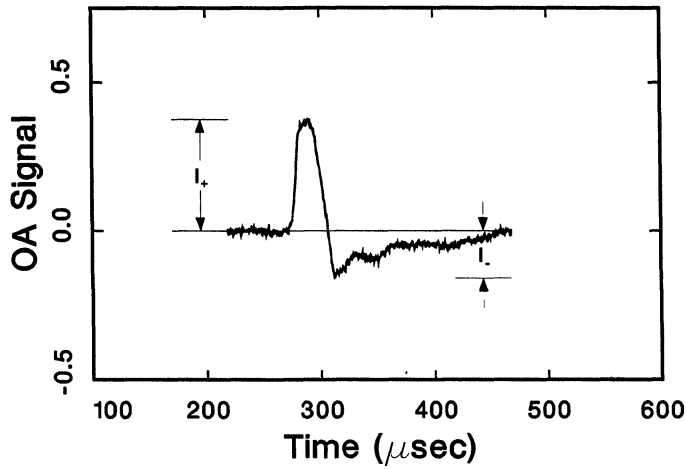

Figure 4 Typical optoacoustic waveform for CH_3Cl + Ar. The condensation and rarefaction amplitudes are denoted as I_- and I_+. Experimental conditions were 2.8 Torr of CH_3Cl and 51.2 Torr of Ar, a laser fluence of 85 mJ cm^{-2} with a beam radius of 0.54 cm, and an average absorbed energy of 100 cm^{-1}. The signal was averaged over 1000 shots.

same as for a source function with pure exponential decay. Assuming that this is the case and using the relation between I_-/I_+ and ε given in Figure 2 of Ref. 7, we obtain the Stern–Volmer plots shown in Figure 6. The effective rate constants for relaxation by Ar, obtained from the slopes of these plots, are listed in Table I with a single standard deviation. Also listed are the effective rate constants determined from the fluorescence and spectrophone experiments. Uncertainties were not quoted in any of those studies.

Table I Measured rate constants[a]

Method	CH_3Cl + Ar	CH_3Br + Ar
TROA[b]	1.32 ± 0.05	3.3 ± 0.2
Spectrophone[c]	0.20	0.25
Fluorescence	0.54[d]	1.29[e]

[a] Units are $Torr^{-1}$ ms^{-1}.
[b] Present results, for a single exponential decay.
[c] Ref. 4a.
[d] Ref. 2.
[e] Ref. 3.

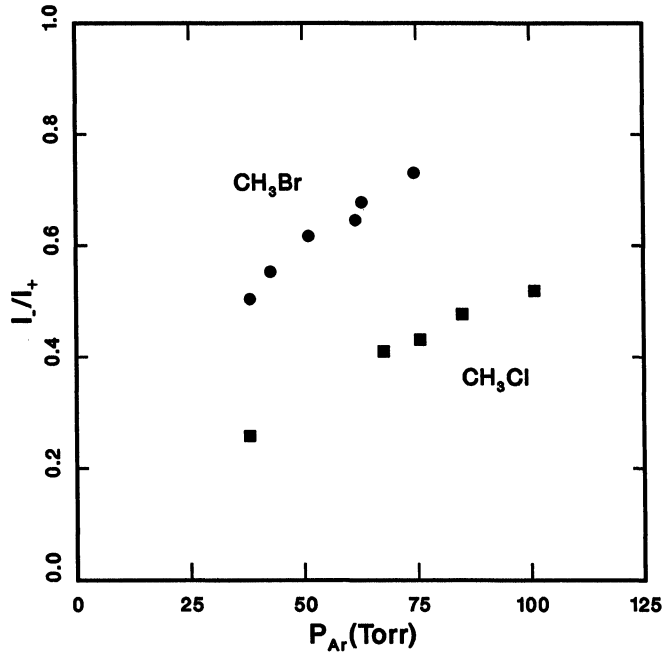

Figure 5 Observed optoacoustic amplitude ratios for CH_3Cl (circles) and CH_3Br (squares) plotted as a function of Ar bath gas pressure.

From the intercepts of Figure 6 we can estimate the effective rate constants for self-relaxation of the excited molecules. For CH_3Cl we obtain a value of 4.0 ± 1.4 ms^{-1} $Torr^{-1}$, as compared with 7.5 ms^{-1} $Torr^{-1}$ obtained in the fluorescence study. Our uncertainty is large because of the long extrapolation to the intercept of zero Ar pressure. For CH_3Br the uncertainty was even greater, but it is still statistically improbable that the rate constant for self-relaxation is larger than the fluorescence value.

VI. DISCUSSION

One conclusion apparent from Table I is that the decay rate of the internal energy in collisions with Ar is more than twice as great as the ν_3 fluorescence decay rate. This is in contradiction to Schuurman and

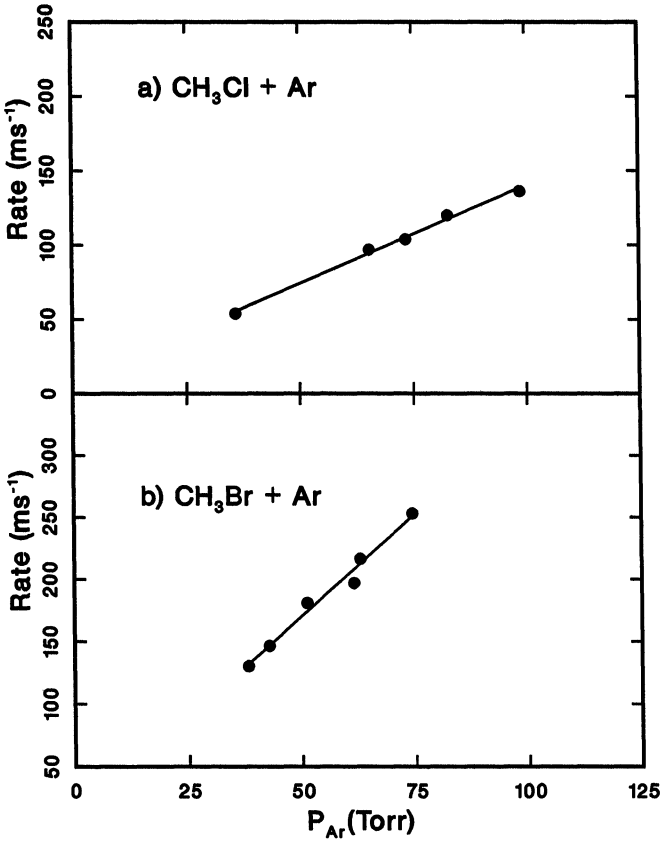

Figure 6 Stern–Volmer plots of CH_3Cl (panel (a)) and CH_3Br (panel (b)) decay rates vs. Ar bath gas pressure. The straight lines are linear least squares fits.

Wegdam who reported rates 3–5 times *smaller* than the fluorescence values. We therefore find no evidence for the rotational bottleneck proposed by them.

Another point for comparison is the ratio of relaxation rate constants for CH_3Br vs. CH_3Cl. For the TROA measurements this ratio is 2.5 ± 0.1, in good agreement with the ratio of 2.4 obtained from IR fluorescence. The faster relaxation observed for CH_3Br is expected since the ν_3 fundamental frequency is smaller for this molecule, necessitating a smaller amount of energy to be removed by V $\rightarrow$ T/R

relaxation. This is consistent with the trend observed in the fluorescence studies for all of the methyl halide-rare gas pairs.[4] In contrast, Schuurman and Wegdam obtained a ratio of only 1.25, and in some instances (e.g. relaxation of CH_3F and CH_3Cl by Kr) they obtained the opposite dependence on ν_3 frequency.

A qualitative explanation for the large rate constants obtained here is that a sizeable fraction of the absorbed energy is rapidly released in $\nu_6 \rightarrow \nu_3$ intermode coupling. For CH_3Cl the $\nu_6 - \nu_3$ gap is 283 cm^{-1} as compared with the 732 cm^{-1} ν_3 fundamental, while for CH_3Br these energies are 344 cm^{-1} and 611 cm^{-1}. The slower V $\rightarrow$ T/R relaxation of ν_3 is thus an example of a vibrational bottleneck, as discussed in the introduction. A difficulty with this explanation is that, as foreseen in Section III, even in the limit of very rapid intermode coupling the pre-exponential factor f_1 would not be large enough to affect I_-/I_+ unless there is some additional source of energy released in the rapid step.

One possible source of additional energy is rotational relaxation in ν_6 and in the ground state. Since in our experiment the laser photon was only 26 cm^{-1} and 17 cm^{-1} larger than $h\nu_6$ for CH_3Cl and CH_3Br, rotational equilibration following the laser pulse adds only a small amount to the total energy release. Another possible source is multiphoton excitation. Experimentally we found that variation of the laser fluence by an order of magnitude in a region of linear absorption[10] had no effect on I_-/I_+ for CH_3Cl + Ar. At the lowest fluence (20.6 mJ/cm^2) the mole fraction of $CH_3Cl(\nu_6)$ was only 2.4 times the value reported in the fluorescence study.[2] This strongly suggests that two-photon excitation was not a major effect in our experiments.

Both intermode coupling and rotational relaxation were invoked to explain thermal lens signals observed by Siebert *et al.*[11] in the relaxation of various small polyatomic molecules including CH_3Cl. For binary mixtures of CH_3Cl and CH_3F they observed the same rate constant obtained in neat CH_3Cl fluorescence measurements, but with an anomalously large intercept, indicating some additional, unknown source of energy release. They attributed this "to a fortuitous combination of V-V, V $\rightarrow$ T/R, and acoustic rates."

From the analysis in Section III it is clear that the simple three-level model cannot reconcile the discrepancy between the TROA and the IR fluorescence measurements. It would therefore appear that additional energy levels must be involved in the "energy map". One

possibility is that anharmonic coupling promotes excitation of overtones and combinations of modes. For example, Zygan-Maus and Fischer[12] have calculated that a Fermi resonance increases k_{IC} for $\nu_1 \rightarrow 2\nu_5$ by two orders of magnitude in CH_3Cl + Ar collisions. They suggest that population of these modes would be even faster in CH_3Cl + CH_3Cl collisions. It is known from the fluorescence studies[2] that ν_1 and ν_4 are rapidly populated, even under conditions of weak excitation. In this context the absence of a fluence effect in our study is problematical.

The amount of extra energy release necessary to explain the TROA rate constants is actually quite small. Returning to the three level model, we calculate that an arbitrary increase of the ν_6 level by as little as 225 cm^{-1} for CH_3Cl and 300 cm^{-1} for CH_3Br could account for the observed decay rates.[13] This could occur, for example, if rotational energy facilitates the ν_6-ν_3 coupling. This would result in a small dynamic barrier which raises the effective upper level of E_6. A similar explanation was proposed for rotational coupling of ν_1 and $2\nu_2$ in SO_2.[14] In that case, however, the coupling is induced by a Fermi resonance at a unique rotational level with an excess energy of ~700 cm^{-1}. Here, since ν_3 and ν_6 have different symmetries, this type of coupling does not occur. A further difficulty is that the enhanced energy release from the top of a rotational barrier must be accompanied by some other endoergic step which would have an opposite effect on the TROA signal. Additional work is clearly needed to reconcile the optoacoustics and the fluorescence experiments.

VII. CONCLUSIONS

Time-resolved optoacoustics measurements showed that the rate of appearance of translational energy in an argon bath gas resulting from the vibrational relaxation of CH_3Cl and CH_3Br is about twice as fast as the IR fluorescence decay rate. There is no evidence for a rotational bottleneck that was proposed in an earlier study. The faster decay rate observed in the acoustics experiment indicates that the relaxation mechanism is more complex than the simple three level model, possibly involving higher vibrational states and/or rotational levels.

Acknowledgements

We wish to thank Prof. George Flynn for a helpful discussion, and Ms. Theresa Reneau

for her assistance with some of the experiments. Helpful comments by the referee are also appreciated. Support by the Office of Basic Energy Sciences of the Department of Energy under grant no. FG02-88ER13827 is gratefully acknowledged.

References

1. S. Hay, F. Shokoohi, S. Callister and C. Wittig, *Chem. Phys. Lett.* **118,** 6 (1985).
2. J. T. Knudtson and G. Flynn, *J. Chem. Phys.* **58,** 2684 (1973).
3. B. L. Earl and A. M. Ronn, *Chem. Phys.* **12,** 113 (1976).
4. (a) J. Schuurman and G. H. Wegdam, *Chem. Phys. Lett.* **73,** 429 (1980); (b) J. A. Schuurman, Ph.D. Thesis (FOM, Amsterdam, 1983).
5. K. M. Beck and R. J. Gordon (submitted).
6. T. J. Wallington, W. Braun, K. M. Beck and R. J. Gordon, *J. Phys. Chem.* **92,** 3839 (1988).
7. K. M. Beck and R. J. Gordon, *J. Chem. Phys.* **87,** 5681 (1987).
8. K. M. Beck, A. Ringwelski and R. J. Gordon, *Chem. Phys. Lett.* **121,** 529 (1985).
9. R. T. Bailey, F. R. Cruickshank, R. Guthrie, D. Pugh and I. J. M. Weir, *Molec. Phys.* **48,** 81 (1983).
10. T. A. Seder and E. Weitz, *J. Chem. Phys.* **104,** 545 (1984).
11. D. R. Siebert, F. R. Grabiner and G. W. Flynn, *J. Chem. Phys.* **60,** 1564 (1974).
12. R. Zygan-Maus and S. F. Fischer, *Chem. Phys.* **41,** 319 (1979).
13. These values are based on an arbitrary estimate of $k_1^{XA} = 10\ \mathrm{ms}^{-1}\ \mathrm{Torr}^{-1}$ for both molecules. A larger choice would reduce the size of the barrier.
14. J. L. Ahl and G. W. Flynn, *J. Phys. Chem.* **87,** 2172 (1983).